Maser and Molecular Line Surveys of Massive Star-forming Regions

Won-Ju Kim[1] and Kee-Tae Kim[2]

Korea Astronomy and Space science Institute (KASI)

[1]deneb@kasi.re.kr, [2]ktkim@kasi.re.kr

ABSTRACT

We made twice a simultaneous 22 GHz H_2O and 44 GHz Class I CH_3OH maser surveys of 103 ultra-compact HII regions (UCHIIs) in 2010 and 2011. We also performed a SiO (J=1-0, v=0) line survey of three samples of massive star-forming regions in different evolutionary stages from 2010 to 2013: 134 infrared dark cores (IRDCs), 135 high-mass proto-stellar objects (HMPOs) and 103 UCHIIs . H_2O and CH_3OH masers were detected in 70 (68%) and 48 (47%) UCHIIs, respectively. Among them, six H_2O and twenty-four CH_3OH masers are new detections. These high detection rates of both masers strongly suggest that their occurrence periods are significantly overlapped with the UCHII phase. CH_3OH masers always have smaller relative velocities than 10 km s^{-1} with respect to the ambient molecular gas, while H_2O masers frequently show larger relative velocities. Eighteen UCHIIs show H_2O maser lines at relative velocities > 30 km s^{-1}. The occurrence and disappearance of H_2O masers are frequent over one-year time interval. In contrast, CH_3OH masers rarely show significant variation in peak velocity, peak intensity, and line shape. The isotropic luminosities of both masers well correlate with the bolometric luminosities of the central stars in the case that data points of low- and intermediate-mass proto-stars are added. They also tend to increase with the 2/6 cm radio continuum luminosities of UCHIIs and the 850 μm continuum luminosity of the parent dense cores. SiO thermal emission was detected in 52 IRDCs (39 %), 22 HMPOs (16 %), and 24 UCHIIs (23 %). Almost SiO emission–detected UCHIIs (96%) have H_2O and/or CH_3OH maser emissions. SiO luminosity is proportional to bolometric luminosity and maser (H_2O and CH_3OH) luminosities. L_{SiO}/L_{bol} ratio tend to decrease as central (proto)stars evolved.

INTRODUCTION

The processes of massive star-forming are poorly understood unlike formation of low-mass star. It is known that the evolution of massive star-forming starts in an infrared dark cloud (IRDC) and then IR emissions are emitted from central condensation region in hot core, which is high-mass proto-stellar object (HMPO). The proto-stellar object eventually reaches main-sequence and forms HII region around central star, which becomes ultra-compact HII region (UCHII). The powerful outflow is important in star formation and generally discovers in IRDC, HMPO and UCHII. H_2O and CH_3OH masers with SiO thermal emission are useful tracer of shock by outflow. H_2O and CH_3OH masers are excited by collisional pumping. H_2O maser are produced in more dense and hot regions than formation regions of CH_3OH. SiO is formed in shocked regions like Si is released from dust grain and conjoin with O (Schilke et al. 1997; Caselli et al. 1997). Si in interstellar medium is observable for ~ 10^4 yr (Pineau des Forets et al. 1997), therefore SiO indicates recent shock activity. We will interpret the evolutionary sequence of massive star-forming by means of H_2O, CH_3OH masers and SiO thermal emission.

OBSERVATION

	H_2O & CH_3OH Observation	SiO thermal Observation
Sources	103 UCHIIs	134 IRDCs, 135 HMPOs, 103 UCHIIs
Telescope	KVN Yonsei 21m	KVN Yonsei/Ulsan/Tamna 21m
Transition	H_2O, 6_{16}-5_{23} (22.23508GHz) CH_3OH, 7_0-6_1 A⁺ (44.06943GHz)	SiO, v=0, J=1-0 (43.423853GHz)
Beam size	130'' @ 22GHz, 65''@44GHz	64''@43GHz
RMS	0.5Jy	30mK
Velocity resolution	0.21 km s^{-1}	1.7 km s^{-1}

※ UCHII : WC89 and KCW94, HMPO : Sridharan et al. (2002) and Zhang et al. (2005), IRDC : Chambers et al. (2009)

RESULTS & DISCUSSION 1: H_2O & CH_3OH masers

Source Group	# of Obs	# of H_2O source (%)	# of CH_3OH source (%)
2010 Obs	103	63 (61%)	44 (43%)
WC89a	52	35 (67%)	25 (48%)
KCW94	51	28 (55%)	19 (37%)
2011 Obs	103	61 (59%)	38 (37%)
WC89a	52	32 (62%)	21 (40%)
KCW94	51	29 (57%)	17 (33%)
Total	103	70 (68%)	48 (47%)
WC89a	52	37 (71%)	26 (50%)
KCW94	51	33 (65%)	22 (43%)

※ WC89 : Wood & Churchwell 1989, KCW94 : Kurtz et al. 1994

✓ Detection Rates

Detection rates of H_2O and CH_3OH for UCHIIs are sufficient high values. The detection rate of H_2O is similar with previous H_2O surveys's rates. So far, Class I CH_3OH masers in previous surveys have been observed toward younger stages than UCHIIs. However, we detected enough CH_3OH masers toward UCHIIs. It is seen that occurrence period of Class I CH_3OH maser considerably overlap with UCHII phase.

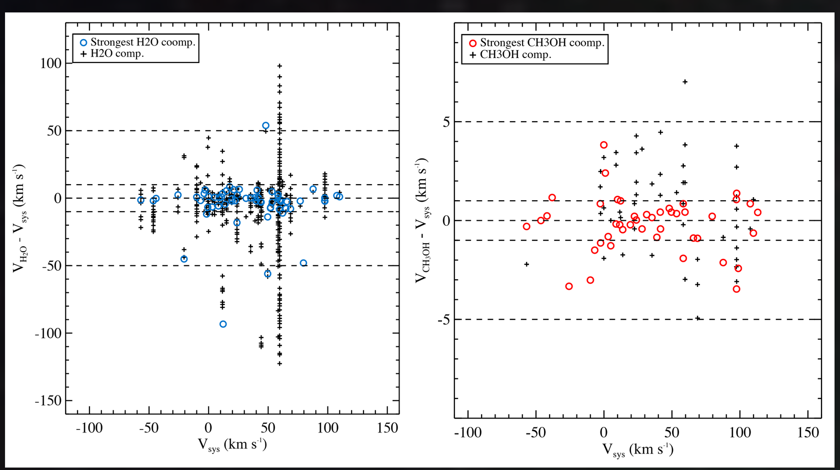

✓ Maser velocities

H_2O masers show a broad velocity distribution while all CH_3OH masers are located within ± 10 km s^{-1}. Usually, H_2O are produced in shock region by high-velocity outflow or jet while CH_3OH are made in interaction region between low-velocity outflow and ambient gas. The H_2O maser shows blue-shifted pattern. The vast majority of the strongest H_2O components (91%) are particularly within 20 km s^{-1}. However, four sources of strongest H_2O components have high relative velocity, which are possible to trace high-velocity jet or outflow. According to the theoretical models, low relative velocity of CH_3OH is because it is destroyed in fast shock over 10 km s^{-1}.

✓ Comparison of Maser Luminosity and Central star properties

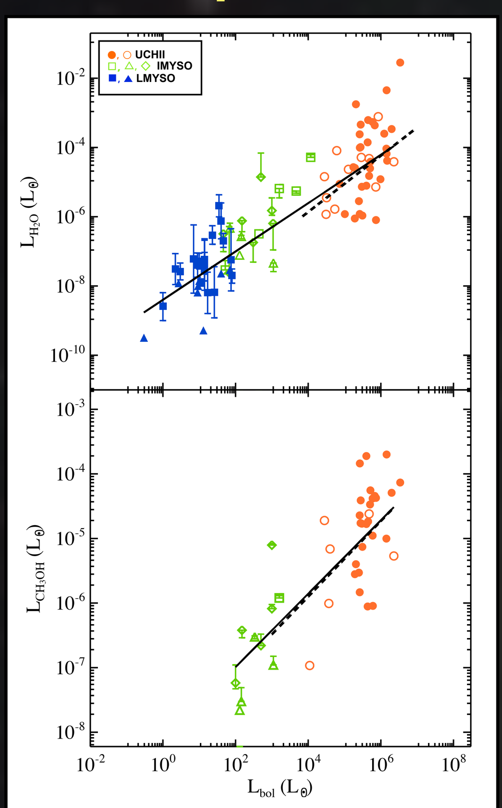

H_2O and CH_3OH maser luminosities are well related with bolometric luminosity for low- (LMYSOs, Furuya et al. 2003) and intermediate-mass YSOs (IMYSOs, Bae et al. 2011) with UCHIIs.
: $L_{H2O} = 3.98\times 10^{-9} (L_{bol})^{0.70}$ with $\rho_{H2O} = 0.90$
: $L_{CH3OH} = 7.44 \times 10^{-9}(L_{bol})^{0.57}$ with $\rho_{CH3OH} = 0.77$

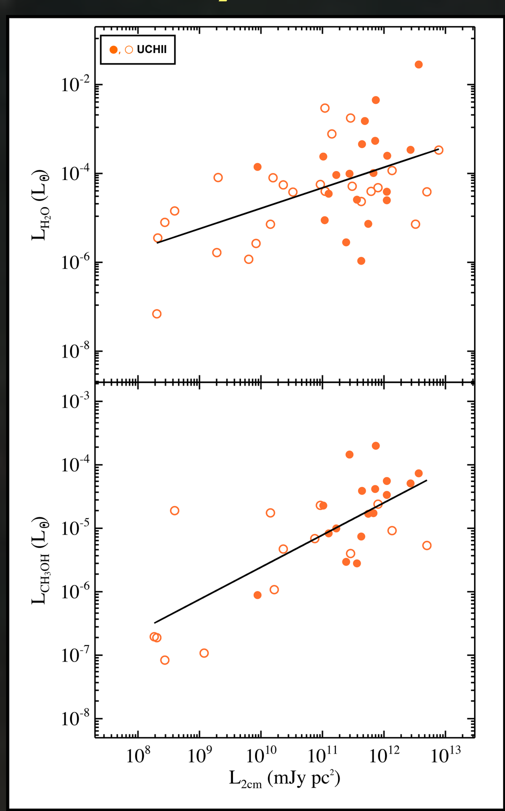

2cm radio continuum luminosity is proportional to L_{H2O} and L_{CH3OH}
: $L_{H2O} = 4.36\times 10^{-10} (L_{2cm})^{0.46}$ with $\rho_{H2O} = 0.52$
: $L_{CH3OH} = 2.18 \times 10^{-11}(L_{2cm})^{0.51}$ with $\rho_{CH3OH} = 0.74$
The radio continuum emission of UCHIIs is mainly originated from HII region around central stars although a part of those comes from radio jets of UCHIIs.

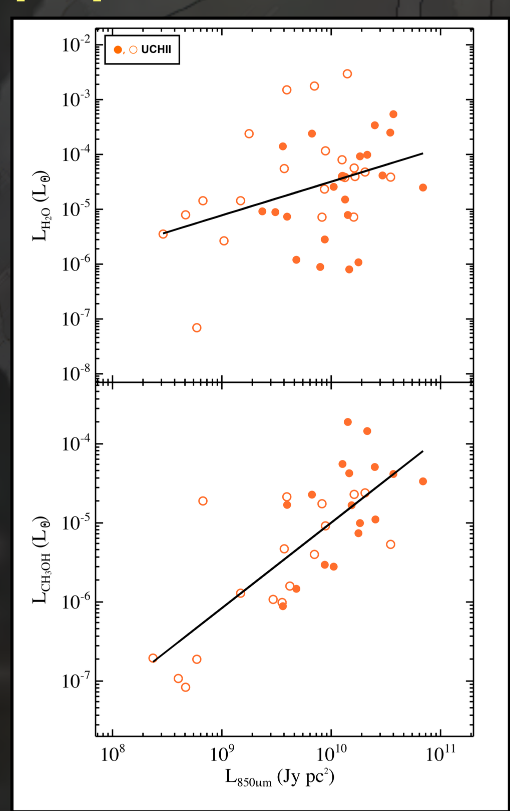

L_{H2O} and L_{CH3OH} are proportional to $L_{850\mu m}$ driven by surrounding dust emission.
: $L_{H2O} = 2.49\times 10^{-11} (L_{850\mu m})^{0.61}$ with $\rho_{H2O} = 0.35$
: $L_{CH3OH} = 1.72 \times 10^{-16}(L_{850\mu m})^{1.08}$ with $\rho_{CH3OH} = 0.76$.
We guess that massive stars made by massive molecular cores are able to produce bright L_{bol} and then induce bright maser luminosities.

✓ L_{Maser} vs. L_{6cm}

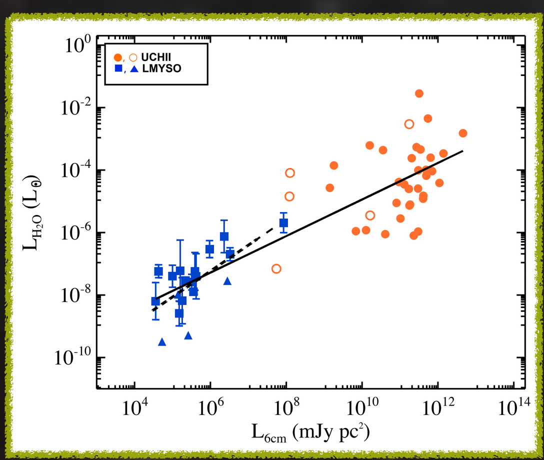

In the case of LMYOs, L_{H2O} is well associated with radio continuum driven by ionized jets or outflows. On the other hand, the radio continuum of UCHIIs is mostly originated from HII region around central stars although a portion of those are induced by radio jets of UCHIIs.

✓ L_{H2O} vs. L_{CH3OH}

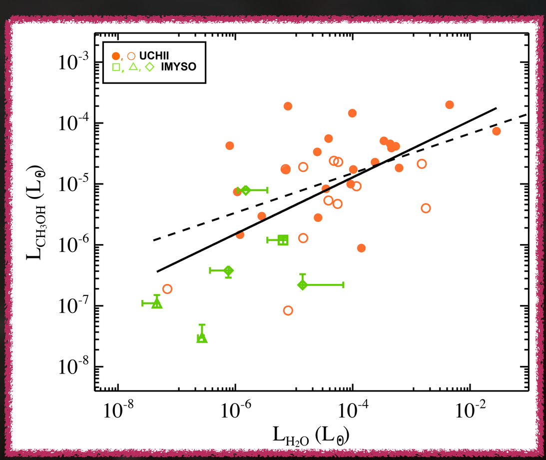

In UCHIIs, H_2O maser luminosity is higher than CH_3OH maser luminosity.: $10^{-7.5} \le L_{H2O}/L_{\odot} \le 10^{-1.5}$ and $10^{-7.5} \le L_{CH3OH}/L_{\odot} \le 10^{-3.5}$.
A relation between L_{H2O} and L_{CH3OH} for UCHIIs shows bad correlation. However, a fitted result of UCHIIs with IMYSOs shows improved a relation.
: $L_{CH3OH} = 9.97 \times 10^{-4}(L_{H2O})^{0.47}$ with $\rho = 0.62$.
It is seen to relate with outflows activity. We also find out that massive central stars produce luminous maser emissions.

SUMMARY

1. H_2O maser emission was detected in 70 (68%) UCHIIs and CH_3OH maser emission in 48 (47%) UCHIIs. Among then, 15 H_2O maser sources and 33 CH_3OH maser sources are new detection.
2. CH_3OH masers always have small (< 10km s^{-1}) relative velocities, while H_2O masers commonly have broader relative velocities with respect to the ambient dense molecular gas.
3. The isotropic luminosities of both masers tend to increase with the bolometric luminosity of central star : $L_{H2O} = 3.98\times 10^{-9} (L_{bol})^{0.70}$ with $\rho_{H2O} = 0.90$ and $L_{CH3OH} = 7.44 \times 10^{-9}(L_{bol})^{0.57}$ with $\rho_{CH3OH} = 0.77$.
4. SiO thermal emission was detected in 52 IRDCs (39 %), 22 HMPOs (16 %), and 24 UCHIIs (23 %). Almost SiO emission–detected UCHIIs (96%) have H_2O and/or CH_3OH maser emissions.
5. Integrated intensity and FWHM of SiO emissions tend to increase with evolutionary sequences.
6. The more luminous SiO sources are associated with higher bolometric luminosity. L_{SiO}/L_{bol} ratio tend to decrease as central (proto)stars evolved.
7. L_{SiO} and SiO column density are related with L_{H2O} and L_{CH3OH} maser luminosities.

RESULTS & DISCUSSION 2: SiO (v=0, J=1-0) thermal emission

✓ Detection Rates & SiO emission

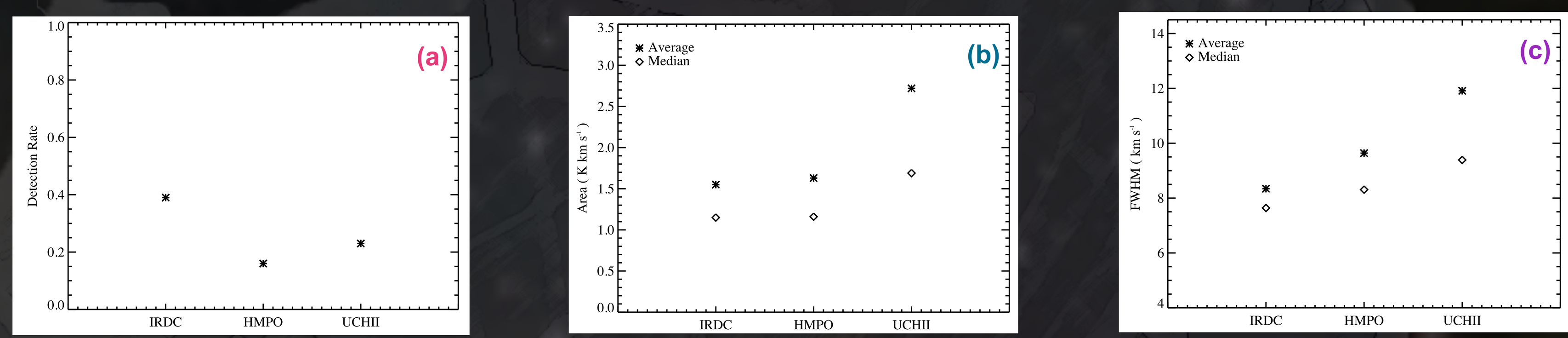

(a) shows detection rates of SiO emission toward IRDC (52/134=39%), HMPO (22/135=16%) and UCHII (24/103=23%). Detection rate of IRDC is the highest and then rate decrease to HMPO. Again, detection rate increase slight to UCHIIs. It is seen that young stage like IRDCs has young SiO outflow because SiO emission has short lifetime of ~ 10^4 years. (b), (c) Integrated intensity and FWHM increase slight as central (proto) stars evolve. We do not know whether the SiO emission of UCHIIs indicates recently produced young outflow or the remainder of old outflow or other factors like cloud-cloud collisions.

✓ Masers Detection Rates for SiO detected sources

Maser / SiO sources	IRDC (52)	HMPO (22)	UCHII (24)
H_2O / SiO	30/52	15/22	22/24
CH_3OH / SiO	39/52	19/22	22/24

In the case of UCHII, the majority (92%) of SiO-detected sources have H_2O or/and CH_3OH masers. In IRDC, although SiO detection rate is the highest among evolutionary stages, H_2O (58%) and CH_3OH (75%) masers detections for SiO-detected sources are less than other stages. The detection rate increases up to 50 % for the 18 UCHIIs with high-velocity H_2O masers. However, the SiO emissions were not detected toward four blue-dominant H_2O sources (V > 50 km s^{-1}) of UCHIIs.

✓ Comparison of SiO thermal Luminosity and Central star properties

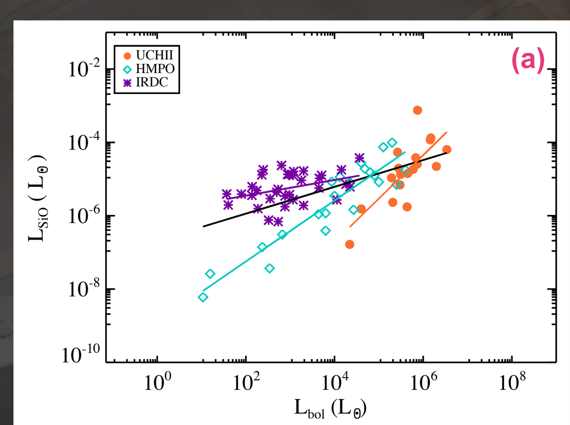

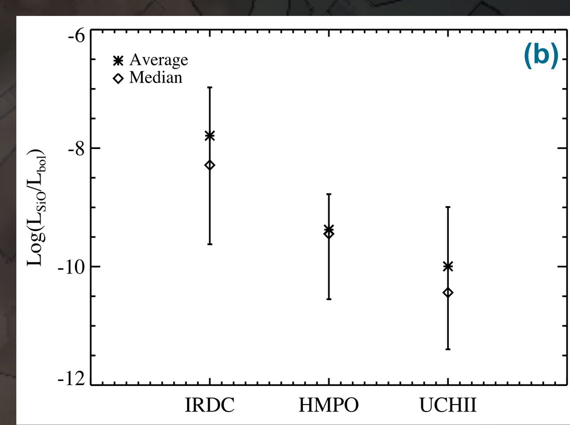

(a) shows to compare L_{bol} with SiO emission luminosity. L_{SiO} of HMPOs and UCHIIs are well associated with L_{bol} while L_{SiO} of IRDC is less correlated with L_{bol}: UCHII, $L_{SiO} = 3.56\times 10^{-12} (L_{bol})^{1.18}$ with $\rho_{SiO} = 0.77$; HMPO, $L_{SiO} = 1.23\times 10^{-09} (L_{bol})^{0.83}$ with $\rho_{SiO} = 0.93$; IRDC, $L_{SiO} = 1.31\times 10^{-06} (L_{bol})^{0.21}$ with $\rho_{SiO} = 0.39$. We find out that more luminous SiO sources are associated with higher bolometric luminosity (Codella et al. 1999). We also find that younger stages have more intense SiO emission then consider identical L_{bol}. (b) presents L_{SiO} / L_{bol} ratio for different evolutionary stages. Like (a), more young stages have higher L_{SiO}/L_{bol} ratio than more old stages (Lopez-Sepulcre et al. 2011).

✓ Comparison of SiO properties and Maser luminosities

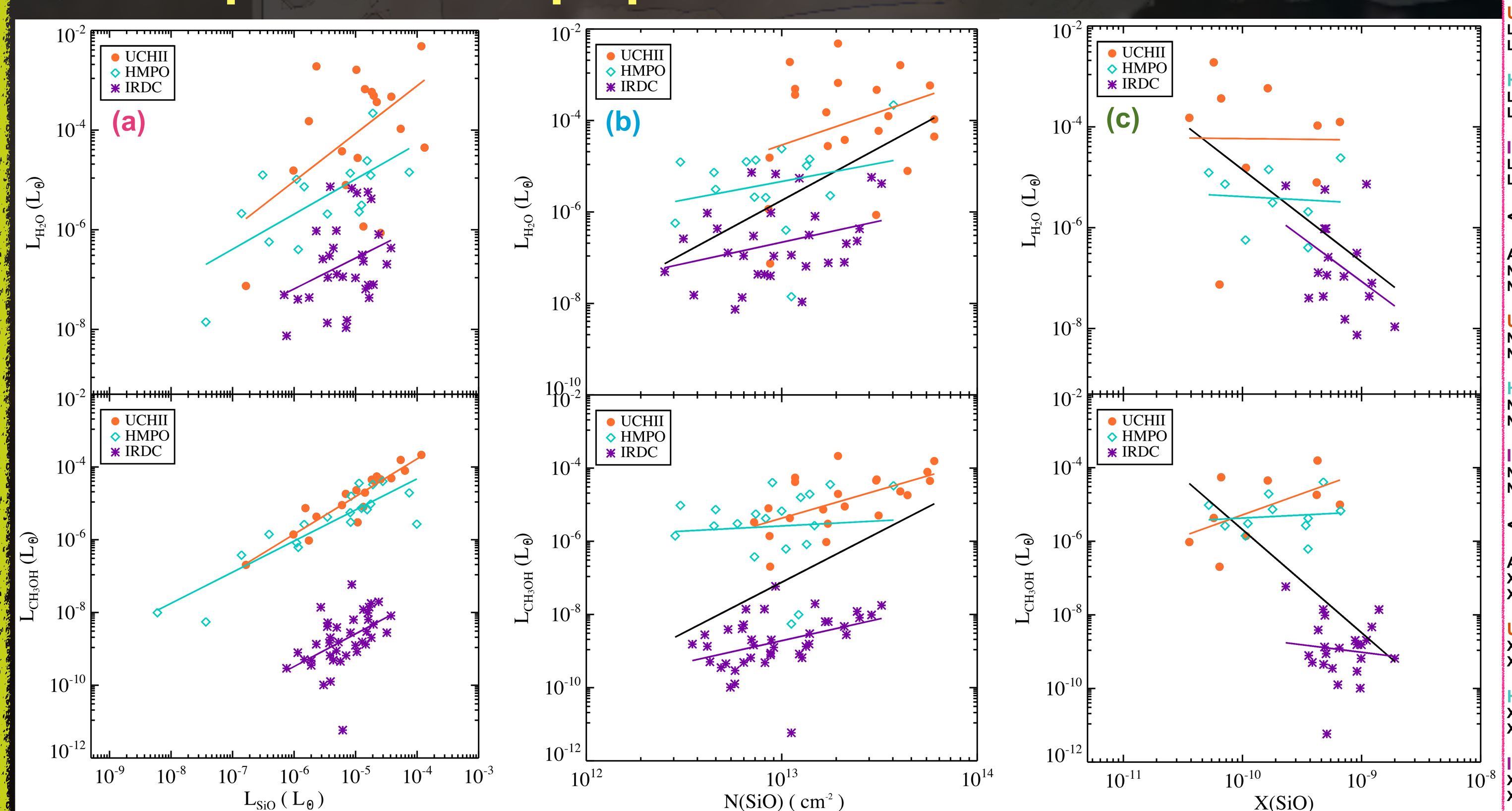

< L_{SiO} vs. L_{maser} >

UCHII
$L_{SiO} = 5.28(L_{H2O})^{0.96}$ with $\rho_{SiO} = 0.50$
$L_{SiO} = 2.33 (L_{CH3OH})^{1.04}$ with $\rho_{SiO} = 0.93$

HMPO
$L_{SiO} = 3.42(L_{H2O})^{0.70}$ with $\rho_{SiO} = 0.68$
$L_{SiO} = 0.13 (L_{CH3OH})^{0.86}$ with $\rho_{SiO} = 0.89$

IRDC
$L_{SiO} = 3.39\times 10^{-4}(L_{H2O})^{0.62}$ with $\rho_{SiO} = 0.33$
$L_{SiO} = 8.20\times 10^{-5} (L_{CH3OH})^{0.90}$ with $\rho_{SiO} = 0.49$

< N(SiO) vs. L_{maser} >

All
$N_{SiO} = 1.58\times 10^{-36}(L_{H2O})^{2.31}$ with $\rho_{SiO} = 0.51$
$N_{SiO} = 1.37\times 10^{-43} (L_{CH3OH})^{2.75}$ with $\rho_{SiO} = 0.43$

UCHII
$N_{SiO} = 4.24\times 10^{-24}(L_{H2O})^{1.45}$ with $\rho_{SiO} = 0.32$
$N_{SiO} = 3.14\times 10^{-26} (L_{CH3OH})^{1.55}$ with $\rho_{SiO} = 0.60$

HMPO
$N_{SiO} = 1.73\times 10^{-16}(L_{H2O})^{0.80}$ with $\rho_{SiO} = 0.25$
$N_{SiO} = 6.17\times 10^{-10}(L_{CH3OH})^{0.28}$ with $\rho_{SiO} = 0.07$

IRDC
$N_{SiO} = 1.76\times 10^{-19}(L_{H2O})^{0.93}$ with $\rho_{SiO} = 0.32$
$N_{SiO} = 6.38\times 10^{-25}(L_{CH3OH})^{1.19}$ with $\rho_{SiO} = 0.41$

< X(SiO) vs. L_{maser} >

All
$X_{SiO} = 7.32\times 10^{-24}(L_{H2O})^{-1.83}$ with $\rho_{SiO} = -0.57$
$X_{SiO} = 1.98\times 10^{-34} (L_{CH3OH})^{-2.80}$ with $\rho_{SiO} = -0.60$

UCHII
$X_{SiO} = 3.20\times 10^{-5}(L_{H2O})^{-0.03}$ with $\rho_{SiO} = -0.01$
$X_{SiO} = 1.97\times 10^{6} (L_{CH3OH})^{1.16}$ with $\rho_{SiO} = 0.56$

HMPO
$X_{SiO} = 2.17\times 10^{-7}(L_{H2O})^{-0.13}$ with $\rho_{SiO} = -0.07$
$X_{SiO} = 1.90\times 10^{-4} (L_{CH3OH})^{0.16}$ with $\rho_{SiO} = 0.12$

IRDC
$X_{SiO} = 1.51\times 10^{-23}(L_{H2O})^{-1.75}$ with $\rho_{SiO} = -0.42$
$X_{SiO} = 2.17\times 10^{-13} (L_{CH3OH})^{-0.41}$ with $\rho_{SiO} = -0.11$

(a), (b) and (c) plot data points of UCHIIs, HMPOs and IRDCs for L_{SiO} against L_{maser}. For (a), L_{H2O} and L_{CH3OH} are proportional to L_{SiO}. L_{CH3OH} is markedly related with L_{SiO}. We guess that is because SiO and CH_3OH are produced in interaction region between outflow and ambient gas (Garay et al. 2002). SiO and CH_3OH are known as tracer of outflow however the SiO emission indicates recently created outflow. We do not know yet whether SiO and CH_3OH indicate identical activity like recently created outflow. For (b), SiO column density also shows similar pattern with Lsio but correlation diminish. For (c), SiO abundance do not show different tendency unlike (a) and (b). We guess that our N_{H2} data are affected from central star contribution like bolometric luminosity. In the case of N_{H2} of IRDCs, we did not reproduce N_{H2} and just brought data of Sanhueza et al. 2012. Therefore, we have to reproduce N_{H2} of IRDCs and to apply new N_{H2} to (c) figures.

References

Wood, D. O. S., & Churchwell, Ed. 1989, ApJS, 69, 831; Kurtz, S., Churchwell, E., & Wood, D. O. S. 1994, ApJS, 91, 659; Garay, G., Mardones, D., Rodrı́guez, L. F., Caselli, P., & Bourke, T. L., 2002, ApJ, 567, 980; Chambers, E. T., Jackson, J. M., Rathborne, J. M., Simon, R, 2009, ApJS, 181, 360.; Sridharan, T. K., Beuther, H., Schilke, P., Menten, K. M., Wyrowski, F., 2002, ApJ, 566, 931; Zhang, Q., Hunter, T. R., Brand, J., Sridharan, T. K., Cesaroni, R., Molinari, S., Wang, J., Kramer, M. 2005, ApJ, 625, 864; Codella, C., Bachiller, R., Reipurth, B., 1999, A&A, 343, 598; Schilke, P., Walmsley, C. M., Pineau des Forets, G., Flower, D. R. 1997, A&A, 321, 293, Caselli et al. 1997, A&A, 322, 296; Pineau des Forets, G., Flower, D. R., Chieze, J.-P., 1997, IAU symp., 182, 199; Lopez-Sepulcre et al. 2011, A&A, 526, L2; Furuya, R. S., Kitamura, Y., Wootten, H. A., Claussen, M. J., & Kawabe, R. 2003, ApJS, 144, 71; Bae, J-H., Kim, K-T., Youn, S-Y., Kim, W-J., Byun, D-Y., Kang, Hyunwoo., & Oh, C. S. 2011. ApJS, 196, 21; Beuther, H., Schilke, P., Menten, K. M., Motte, F., Sridharan, T. K., Wyrowski, F., 2002, ApJ, 566, 945; Sanhueza, P., Jackson, J. M., Foster, J. B., Garay, G., Silva, A., Finn, S. C., ApJ, 756, 60; Di Francesco, J., Johnstone, D., Kirk, H., MacKenzie, T., Ledwosinska, E., 2008, ApJS, 175, 277